Heterometallic Au-Pt-Hg and Au-Pt-Hg-Co Phosphine-Stabilized Cluster Compounds. X-ray Crystal and Molecular Structure of $[(PPh_3)Pt(AuPPh_3)_6(HgNO_3)]NO_3$

Rachael A. T. Gould and Louis H. Pignolet*

Department of Chemistry, University of Minnesota Minneapolis, Minnesota 55455

Received July 30, 1993®

The synthesis and characterization of a series of new mercury containing platinum-gold cluster compounds are reported. The compound $[(PPh_3)Pt(AuPPh_3)_6(HgNO_3)](NO_3)$ (**1**(NO_3)) was prepared by the addition of metallic mercury to $[(PPh_3)Pt(AuPPh_3)_6](NO_3)_2$. Halide derivatives of **1** were prepared by reaction with halides X^- (X = Cl, Br, I) to give the series $[(PPh_3)Pt(AuPPh_3)_6(HgX)]^+$ (**2**). Metallic mercury can be displaced from **1** by reaction with CO (1 atm) giving the known carbonyl adduct $[(PPh_3)(CO)Pt(AuPPh_3)_6]^{2+}$. This reaction is reversible. The first tetrametallic derivatives of Pt-centered, gold cluster compounds $[(PPh_3)Pt(AuPPh_3)_6(HgCo(CO)_4)]^+$ (**3**), and $[(PPh_3)Pt(AuPPh_3)_5(HgCo(CO)_4)_2]^+$ (**4**), have been prepared by reaction of $NaCo(CO)_4$ with **1** and $[(PPh_3)Pt(AuPPh_3)_5(HgNO_3)_2]^+$, respectively. Compound **1** has been characterized by single crystal X-ray diffraction. **1** crystalizes as a $(C_2H_5)_2O\cdot(CH_3)_2CO$ solvate with the following crystal data: monoclinic $P2_1/c$, a = 24.968 (7) Å, b = 15.848 (9) Å, c = 30.60 (1) Å, β = 92.69 (3)°, V = 12,093 Å^3, Z = 4, and residuals R = 0.077 and R_w = 0.071 for 7722 observed reflections and 462 variables and Mo Kα radiation, at −100 °C. The $PPtM_7$ core of **1** has an unusual geometry that is best described as being between the limits of a Pt-centered, icosahedral fragment and a cube. Clusters are known with both of these limiting geometries and although **1** is inbetween, it is spheroidal in agreement with its 18-electron count.

Introduction

The study of phosphine stabilized, mixed-metal-gold cluster compounds has resulted in the preparation of a number of new polymetallic clusters which show interesting structural and reactivity properties.[1-5] Several exciting, recent developments in this area are the preparation of the supracluster $[Pt_2(AuPPh_3)_{10}Ag_{13}Cl_7]$[6] and the discovery that several of the platinum-gold clusters (notably $[Pt(AuPPh_3)_8]^{2+}$) are excellent catalysts for H_2 activation in solution and in the solid state.[7,8] Mixed-metal clusters are of general interest as models of the surfaces of bi- and polymetallic heterogeneous catalysts.[9] A study of such clusters will also provide a better understanding of metal-metal bonding and the synergism often observed in catalytic reactions.[9,10] We are therefore interested in developing systematic methods of preparing heterometallic cluster compounds.

Platinum-centered clusters of the general formulation $[L_yPt(AuPPh_3)_x(ML'_z)]^{n+}$ (L and L' are ligands (such as PR_3, CO, halide, H, and NO_3), M is a metal (such as Ag, Sn, Cu, and Hg), x = 2-8, y = 0-2, and z = 0-3) have been the most extensively studied.[1-8] Structural and reactivity properties of this general class of cluster compound have been rationalized with the use of electron counting rules.[1-5,11,12] For example, the 16-electron cluster $[(PPh_3)Pt(AuPPh_3)_6]^{2+}$ has a flattened, toroidal geometry and reacts with two-electron donors to give 18-electron clusters with spheroidal geometry. Examples are the reactions of $[(PPh_3)Pt(AuPPh_3)_6]^{2+}$ with CO and $Hg_2(H_2O)_2(NO_3)_2$ to give the spheroidal clusters $[(PPh_3)(CO)Pt(AuPPh_3)_6]^{2+}$ and $[(PPh_3)Pt(AuPPh_3)_5(HgNO_3)_2]^+$, respectively.[5] Most of the structures of the 18-electron, spheroidal clusters (including the two above) can be described as Pt-centered, icosahedral fragments; however, there are examples of other spheroidal geometries. Examples are $[Pt(AuPPh_3)_8(Hg)_2]^{4+}$ and $[(PPh_3)(H)Pt(AuPPh_3)_7]^{2+}$, which have bicapped square-antiprismatic and distorted cubic structures, respectively.[13,14]

The focus of this paper is on the preparation of mercury-containing Pt-Au cluster compounds and a study of their

* Abstract published in *Advance ACS Abstracts,* December 1, 1993.

(1) Steggerda, J. J. *Comments Inorg. Chem.* **1991**, *11*, 113.
(2) Mueting, A. M.; Bos, W.; Alexander, B. D.; Boyle, P. D.; Casalnuovo, J. A.; Balaban, S.; Ito, L. N.; Johnson, S. M.; Pignolet, L. H. *New J. Chem.* 1988, *12*, 505.
(3) Schoondergang, M. F. J.; Bour, J. J.; Schlebos, P. P. J.; Vermeer, A. W. P.; Bosman, W. P.; Smits, J. M. M.; Beurskens, P. T.; Steggerda, J. J. *Inorg. Chem.* **1991**, *30*, 4704 and references cited therein.
(4) Schoondergang, M. F. J.; Bour, J. J.; van Strijdonck, G. P. F.; Schlebos, P. P. J.; Bosman, W. P.; Smits, J. M. M.; Beurskens, P. T.; Steggerda, J. J. *Inorg. Chem.* **1991**, *30*, 2048.
(5) Ito, L. N.; Felicissimo, A. M. P.; Pignolet, L. H. *Inorg. Chem.* **1991**, *30*, 387.
(6) This cluster has recently been prepared by the Steggerda research group (Kappen, T. G. M. M.; Schlebos, P. P. J.; Bour, J. J.; Bosman, W. P.; Smits, J. M. M.; Beurskens, P. T.; Steggerda, J. J. Submitted for publication in *Inorg. Chem.*) and consists of two Pt-centered $Pt(AuPPh_3)_5$-Ag_7 icosahedra sharing a common Ag vertex with five Cl atoms bridging between Ag atoms of the two icoshedra and two bound to Ag atoms at oppposite ends of the cluster. The structure is similar to that of the vertex-shared biicosahedral $Au_{13}Ag_{12}$ cluster reported by Teo (Teo, B. K.; Zhang, H.; Shi, X. *Inorg. Chem.* **1990**, *29*, 2083).
(7) Aubart, M. A.; Pignolet, L. H. *J. Am. Chem. Soc.* **1992**, *114*, 7901.
(8) Kappen, T. G. M. M.; Bour, J. J.; Schlebos, P. P. J.; Roelofsen, A. M.; van der Linden, J. G. M.; Steggerda, J. J.; Aubart, M. A.; Krogstad, D. A.; Schoondergang, M. F. J.; Pignolet, L. H. *Inorg. Chem.* **1993**, *32*, 1074.
(9) Braunstein, P.; Rose, J. In *Stereochemistry of Organometallic and Inorganic Compounds*, Bernal, I. Ed.; Elsevier: Amsterdam, The Netherlands, 1988; Vol 3. Saillard, J-Y.; Hoffman, R. *J. Am. Chem. Soc.*, **1984**, *106*, 2006. Van Gastel, F.; Corrigan, J. F.; Doherty, S.; Taylor, N. J.; Carty, A. J. *Inorg. Chem.* **1992**, *31*, 4492 and references cited therein.
(10) Sachdev, A.; Schwank, J. *J. Catal.* **1989**, *120*, 353. Sermon, P. A.; Thomas, J. M.; Keryou, K.; Millward, G. R. *Angew. Chem., Int. Ed. Engl.* **1987**, *26*, 918. Yates, R. C.; Somorjai, G. A. *J. Catal.* **1987**, *103*, 208. Sinfelt, J. H. *Bimetallic Catalysts*; Wiley: New York, 1985.
(11) Mingos, D. M. P.: Wales, D. J. *Introduction to Cluster Chemistry*; Prentice Hall: Englewood Cliffs, NJ, 1993.
(12) Mingos, D. M. P.; Johnston, R. L. *Struct. Bonding* **1987**, *68*, 29. Stone, A. J. *Inorg. Chem.* **1981**, *20*, 563. Kanters, R. P. F.; Schlebos, P. P. J.; Bour, J. J.; Bosman, W. P.; Behm, H. J.; Steggerda, J. J. *Inorg. Chem.* **1988**, *27*, 4034. Bour, J. J.; Kanters, R. P. F.; Schlebos, P. P. J.; Bosman, W. P.; Behm, H.; Beurskens, P. T.; Steggerda, J. J. *Recl.: J. R. Neth. Chem. Soc.* **1987**, *106*, 157. Bour, J. J.; Kanters, R. P. F.; Schlebos, P. P. J.; Steggerda, J. J. *Recl.: J. R. Neth. Chem. Soc.* **1988**, *107*, 211. Kanters, R. P. F.; Schlebos, P. P. J.; Bour, J. J.; Bosman, W. P.; Smits, J. M. M.; Beurskens, P. T.; Steggerda, J. J. *Inorg. Chem.* **1990**, *29*, 324.
(13) Kanters, R. P. F.; Bour, J. J.; Schlebos, P. P. J.; Bosman, W. P.; Behm, H.; Steggerda, J. J.; Ito, L. N.; Pignolet, L. H. *Inorg. Chem.* **1989**, *28*, 2591.
(14) Bour, J. J.; van den Berg, W.; Schlebos, P. P. J.; Kanters, R. P. F.; Schoondergang, M. F. J.; Bosman, W. P.; Smits, J. M. M.; Beurskens, P. T.; Steggerda, J. J.; van den Sluis, P. *Inorg. Chem.* **1990**, *29*, 2971.

0020-1669/94/1333-0040$04.50/0

structural and reactivity properties. Although metallic mercury has been used as a reagent to prepare mixed-metal cluster compounds,[15-18] the use of Hg(II) and Hg(I) (Hg_2^{2+}) compounds is more common.[18-22] We have obtained different Pt–Au–Hg cluster compounds with use of metallic Hg compared with Hg(I) reagents. One of our interests in developing Pt–Au–Hg chemistry is the possibility of preparing larger supraclusters by linking together smaller *building block* clusters with Hg or Hg_2 bridges. It is well established that mercury is an excellent metal to bridge between various transition metals in clusters.[15-23] We are also interested in exploring the isolobal relationship between Au(I), Hg(II), and H^+.[22] This is especially relevant in light of the recent discovery that some Pt–Au clusters react with H_2 to form dihydrides and function as excellent H_2–D_2 equilibration catalysts.[7,8] Finally, we are interested in studying the effect of the incorporation of different metal types on catalytic activity and selectivity. In this paper we report the synthesis and characterization of the new clusters $[(PPh_3)Pt(AuPPh_3)_6(HgX)]^+$, where X = NO_3, Cl, Br, and I, and the first tetrametallic derivatives of Pt-centered, gold cluster compounds $[(PPh_3)Pt(AuPPh_3)_6(HgCo(CO)_4)]^+$ and $[(PPh_3)Pt(AuPPh_3)_5(HgCo(CO)_4)_2]^+$.

Experimental Section

Physical Measurements and Reagents. ^{31}P NMR spectra were recorded at 121.4 MHz with use of a Varian VXR 300-MHz spectrometer. ^{31}P NMR spectra were run with proton decoupling and shifts are reported in ppm relative to internal standard trimethylphosphate (TMP) with positive shifts downfield. NMR spectra were run with use of acetone solvent at ambient temperature (20 °C) unless noted otherwise. Infrared spectra were recorded in the solid state on a Perkin-Elmer Model 1600 FT-IR spectrometer with use of CsI pellets. Conductivity measurements were made with use of a Yellow Springs Model 35 conductance meter. Compound concentrations used in the conductivity experiments were 3 × 10^{-4} M in CH_3CN solution. FABMS measurements were carried out with use of a VG Analytical, Ltd. 707E-HF high resolution, double-focusing mass spectrometer equipped with a VG 11/250 data system. FABMS samples were introduced in a *m*-nitrobenzyl alcohol matrix. Microanalyses were carried out by Analytische Laboratories Engelskirchen, Germany. ICP analyses of DMSO solutions of the clusters were carried out with use of a Plasma 200 ICP A-E spectrometer with $Pt(AuPPh_3)_8(NO_3)_2$ used as a reference. Solvents were dried and distilled prior to use. $Na[Co(CO)_4]$[24] and the cluster compounds $[(PPh_3)Pt(AuPPh_3)_5(HgNO_3)_2](NO_3)$[5] and $[(PPh_3)Pt(AuPPh_3)_6](NO_3)_2$[25] were prepared as described in the literature. All manipulations were carried out under a purified N_2 atmosphere with use of standard Schlenk techniques.

Preparation of the Compounds. $[(PPh_3)Pt(AuPPh_3)_6(HgNO_3)](NO_3)$ ($1(NO_3)$). One drop of metallic mercury (about 80 mg) was added to a stirred acetone solution (8 mL) of $[(PPh_3)Pt(AuPPh_3)_6](NO_3)_2$ (74 mg, 0.022 mmol) at room temperature. The reaction mixture became more red in color within the first 10 min. After overnight stirring, the acetone solution was filtered through diatomaceous earth to remove unreacted Hg metal. The resulting clear red filtrate was reduced in volume to approximately 6 mL and 10 mL of diethyl ether added. Small red crystals formed after this mixture was allowed to stand for 12 h. These were collected and washed with 3 × 5 mL portions of diethyl ether and dried *in vacuo*. Yield: 0.0728 g (93%) after recrystallization from an acetone–diethyl ether solvent mixture. X-ray quality crystals were obtained by layering a concentrated acetone solution with diethyl ether. The dark red crystals are soluble in halogenated solvents, CH_3CN, CH_3OH, and acetone and insoluble in saturated hydrocarbons and diethyl ether. ^{31}P NMR: δ 60.5 (septet with ^{195}Pt satellites, $^3J_{P-P}$ = 31.8 Hz, $J_{^{195}Pt-P}$ = 3070 Hz, $^2J_{^{199}Hg-P}$ unobserved, int = 1), δ 50.5 (doublet with ^{195}Pt and ^{199}Hg satellites, $^3J_{P-P}$ = 31.8 Hz, $^2J_{^{195}Pt-P}$ = 462 Hz, $^3J_{^{199}Hg-P}$ = 655 Hz, int = 6). IR: $\nu(NO_3)$ 1340 cm^{-1} (br) (unbound) and 1270 cm^{-1} (bound). The measured equivalent conductance (202 cm^2 mho mol^{-1}) is higher than expected for a 1:1 electrolyte (typical values found in our lab for similar +1 PtAu cluster cations are 80–130 cm^2 mho mol^{-1} and the range 180–230 cm^2 mho mol^{-1} is observed for +2 cations[2,5,25]) indicating that the cluster is dissociated to $[(PPh_3)Pt(AuPPh_3)_6(Hg)]^{2+}$ in CH_3CN solution. ICP analysis: Pt:Au:P = 1:6.09:7.01. Anal. Calcd for $PtAu_6HgP_7C_{126}H_{105}N_2O_6$: C, 42.78; H, 2.99; N, 0.79. Found: C, 42.83; H, 2.89; N, 0.74. FABMS: obsvd *m/z* 3475.8 {calcd 3475.5 for $[(PPh_3)Pt(AuPPh_3)_6(HgNO_3) = M]^+$}, 3212.5 {calcd 3212.9 for $[M - (HgNO_3)]^+$}, 3012.2 {calcd 3012.6 for $[M - (HgPPh_3)]^+$}, 2950.2 {calcd 2950.6 for $[M - (HgNO_3PPh_3)]^+$}, 2752.1 {calcd 2753.6 for $[M - (AuPPh_3HgNO_3)]^+$}, 2687.8 {calcd 2687.9 for $[M - (HgNO_3(PPh_3)_2)]^+$}, 2490.7 {calcd 2491.3 for $[M - (HgNO_3PPh_3AuPPh_3)]^+$}.

$[(PPh_3)Pt(AuPPh_3)_6(HgX)](NO_3)$ ($2(NO_3)$, X = Cl). $[(PPh_3)Pt(AuPPh_3)_6(HgCl)](NO_3)$ was prepared by the reaction of $1(NO_3)$ (41 mg, 0.0116 mmol) with $Et_4NCl{\cdot}H_2O$ (2.1 mg, 0.0127 mmol) in 10 mL of methanol. The solids dissolved immediately producing an orange solution. After this solution was stirred for 2 h, the volume of the reaction mixture was reduced to approximately 5 mL and filtered through diatomaceous earth. The resulting clear orange-red filtrate was evaporated to dryness. The orange residue was redissolved in 3 mL of acetone and 5 mL of diethyl ether added. Orange crystals were collected after standing overnight and were washed with diethyl ether and dried *in vacuo*. Yield: 0.026 g (63%) after recrystallization. The bright orange solid is soluble in halogenated solvents, CH_3CN, CH_3OH, and acetone and insoluble in saturated hydrocarbons and diethyl ether. ^{31}P NMR: δ 65.4 (septet with ^{195}Pt satellites, $^3J_{P-P}$ = 35.5 Hz, $J_{^{195}Pt-P}$ = 2813 Hz, $^2J_{^{199}Hg-P}$ unobserved, int = 1), δ 49.7 (doublet with ^{195}Pt and ^{199}Hg satellites, $^3J_{P-P}$ = 35.5 Hz, $^2J_{^{195}Pt-P}$ = 468 Hz, $^3J_{^{199}Hg-P}$ = 566 Hz, int = 6). IR: $\nu(NO_3)$ 1340 cm^{-1} (br). Equivalent conductance 199 cm^2 mho mol^{-1}. FABMS: obsvd *m/z* 3448.9 {calcd 3448.9 for $[(PPh_3)Pt(AuPPh_3)_6(HgCl) = M]^+$}, 3475.4 {calcd 3475.5 for $[M - (Cl)+NO_3)]^+$}, 3212.9 {calcd 3212.9 for $[M - (HgCl)]^+$}, 3012.4 {calcd 3012.6 for $[(M + (NO_3)-(HgClPPh_3)]^+$}, 2950.4 {calcd 2950.6 for $[M - (HgClPPh_3)]^+$}, 2753.5 {calcd 2753.6 for $[M - (AuPPh_3HgCl)]^+$}, 2688.3 {calcd 2687.9 for $[M - (HgCl(PPh_3)_2)]^+$}.

$[(PPh_3)Pt(AuPPh_3)_6(HgX)](PF_6)$ ($2(PF_6)$, X = Cl). $[(PPh_3)Pt(AuPPh_3)_6(HgCl)](PF_6)$ was prepared by dissolving 10 mg (0.0028 mmol) of $2(NO_3)$, X = Cl, in 3 mL of acetone and adding an acetone solution (1 mL) of NH_4PF_6 (2.4 mg, 0.015 mmol). After being stirred for 1 h, the acetone solution was evaporated to dryness under reduced pressure and the orange residue redissolved in 5 mL of methanol. Reduction of the methanol solution to 1 mL yielded orange-red microcrystals. The crystals were collected, washed with diethyl ether, and dried. Yield: 7.7 mg (75%) after recrystallization. Spectral data are the same as for $2(NO_3)$, X = Cl, with $\nu(PF_6)$ 840 cm^{-1} and no $\nu(NO_3)$ bands in the IR and a septet at δ −146 ppm in the ^{31}P NMR corresponding to the presence of PF_6^-. FABMS: obsvd *m/z* 3448.7 {calcd 3448.9 for $[(PPh_3)Pt(AuPPh_3)_6(HgCl) = M]^+$}, 3357.7 {calcd 3357.9 for $[M + (PF_6) - (HgCl)]^+$}, 3212.6 {calcd 3212.9 for $[M - (HgCl)]^+$}, 2950.3 {calcd 2950.6 for $[M - (HgClPPh_3)]^+$}, 2753.3 {calcd 2753.6 for $[M - (AuPPh_3HgCl)]^+$}, 2688.0 {calcd 2687.9 for $[M - (HgCl(PPh_3)_2)]^+$}.

$[(PPh_3)Pt(AuPPh_3)_6(HgBr)](NO_3)$ ($2(NO_3)$, X = Br). $[(PPh_3)Pt(AuPPh_3)_6(HgBr)](NO_3)$ was prepared by dissolving 44.4 mg (0.0126 mmol) of $1(NO_3)$ in 10 mL of methanol and adding a methanol solution (2 mL) of 2.9 mg (0.014 mmol) Et_4NBr. After being stirred for 40 min, the solution was evaporated to dryness. The orange residue was redissolved in 8 mL of acetone, and dark orange-red crystals resulted upon the addition of 6–8 mL of diethyl ether. Yield: 20 mg (45%) after recrystallization. The dark orange solid is soluble in halogenated solvents, CH_3CN, CH_3-

(15) Schoettel, G.; Vittal, J. J.; Puddephatt, R. J. *J. Am. Chem. Soc.* **1990**, *112*, 6400.
(16) Gade, L. H.; Johnson, B. F. G.; Lewis, J.; Conole, G.; McPartlin, M. *J. Chem. Soc., Dalton Trans.* **1992**, 3249 and references cited therein.
(17) Albinati, A.; Moor, A.; Pregosin, P. S.; Venanzi, L. M. *J. Am. Chem. Soc.* **1982**, *104*, 7672.
(18) Burtlitch, J. M. In *Comprehensive Organometallic Chemistry*; Wilkinson, G., Stone, F. G. A., Abel, E. W., Eds.; Pergamon: Oxford, U.K., 1982; Vol. 6, p 983.
(19) Gade, L. H. *Angew. Chem., Int. Ed. Engl.* **1993**, *32*, 24.
(20) Deeming, A. J. *J. Cluster Sci.* **1992**, *3*, 347.
(21) Dean, P. A. W. In *Comprehensive Organometallic Chemistry*; Wilkinson, G., Gillard, R. D., McCleverty, J. A., Eds.; Pergamon: Oxford, U.K., 1987; Vol. 2, p 1.
(22) Braunstein, P.; Rose, J.; Tiripicchio, A.; Camellini, M. T. *J. Chem. Soc., Dalton Trans.* **1992**, 911 and references cited therein.
(23) See, for example: Braunstein, P.; Knorr, M.; Tiripicchio, A.; Camellini, M. T. *Inorg. Chem.* **1992**, *31*, 3685. Braunstein, P.; Rossell, O.; Seco, M.; Torra, I.; Solans, X.; Miravitlles, C. *Organometallics* **1986**, *5*, 1113. Tyler, S. J.; Burtlitch, J. M. *J. Organomet. Chem.* **1989**, *361*, 231. Albinati, A.; Dahmen, K. H.; Demartin, F.; Forward, J. M.; Longley, C. J.; Mingos, D. M. P.; Venanzi, L. M. *Inorg. Chem.* **1992**, *31*, 2223. Yamamoto, Y.; Yamazaki, H. *J. Chem. Soc., Dalton Trans.* **1989**, 2161. Cecconi, F.; Ghilardi, C. A.; Midollini, S.; Moneti, S. *J. Chem. Soc., Dalton Trans.* **1983**, 349.
(24) Dighe, S. V.; Orchin, M. *Inorg. Chem.* **1962**, *1*, 965.
(25) Ito, L. N.; Sweet, J. D.; Mueting, A. M.; Pignolet, L. H.; Schoondergang, M. F. J.; Steggerda, J. J. *Inorg. Chem.* **1989**, *28*, 3696.

OH, and acetone and insoluble in saturated hydrocarbons and diethyl ether. ^{31}P NMR: δ 65.3 (septet with ^{195}Pt satellites, $^3J_{P-P}$ = 35.4 Hz, $J_{^{195}Pt-P}$ = 2830 Hz, $^2J_{^{199}Hg-P}$ unobserved, int = 1), δ 49.3 (doublet with ^{195}Pt and ^{199}Hg satellites, $^3J_{P-P}$ = 35.4 Hz, $^2J_{^{195}Pt-P}$ = 470 Hz, $^3J_{^{199}Hg-P}$ = 564 Hz, int = 6). IR: $\nu(NO_3)$ 1340 cm^{-1} (br) (unbound). Equivalent conductance: 154 cm^2 mho mol^{-1}. FABMS: obsvd *m/z* 3493.5 {calcd 3493.4 for $[(PPh_3)Pt(AuPPh_3)_6(HgBr) = M]^+$}, 3314.6 {calcd 3314.6 for $[(PPh_3)Pt(AuPPh_3)_5(HgBr)_2]^+$} (see discussion for explanation), 3212.7 {calcd 3212.9 for $[M - (HgBr)]^+$}, 3030.3 {calcd 3030.5 for $[M - (PPh_3Hg)]^+$}, 3012.4 {calcd 3012.6 for $[M + (NO_3)\text{-}(HgBrPPh_3)]^+$}, 2950.4 {calcd 2950.6 for $[M - (HgBrPPh_3)]^+$}, 2753.1 {calcd 2753.6 for $[M - (AuPPh_3HgBr)]^+$}, 2688.4 {calcd 2687.9 for $[M - (HgBr(PPh_3)_2)]^+$}.

$[(PPh_3)Pt(AuPPh_3)_6(HgI)](NO_3)$ (2(NO_3), X = I). $[(PPh_3)Pt(AuPPh_3)_6(HgI)](NO_3)$ was prepared by dissolving 46 mg (0.013 mmol) of 1(NO_3) and 5.2 mg (0.014 mmol) of Bu_4NI in 10 mL of methanol. After being stirred for 35 min, the orange-red solution was evaporated to dryness and the residue redissolved in 2 mL of acetone. Addition of 4 mL of diethyl ether resulted in the formation of small orange crystals. After the mixture was allowed to stand for 24 h, the crystals were collected, washed with diethyl ether, and dried. Yield: 34.4 mg (75%) after recrystallization. The dark orange-red powder is soluble in halogenated solvents, CH_3CN, CH_3OH, and acetone and insoluble in saturated hydrocarbons and diethyl ether. ^{31}P NMR: δ 65.8 (septet with ^{195}Pt satellites, $^3J_{P-P}$ = 35.4 Hz, $J_{^{195}Pt-P}$ = 2813 Hz, $^2J_{^{199}Hg-P}$ unobserved, int = 1), δ 49.0 (doublet with ^{195}Pt and ^{199}Hg satellites, $^3J_{P-P}$ = 35.4 Hz, $^2J_{^{195}Pt-P}$ = 471 Hz, $^3J_{^{199}Hg-P}$ = 544 Hz, int = 6). IR: $\nu(NO_3)$ 1340 cm^{-1} (br) (unbound). Equivalent conductance: 110 cm^2 mho mol^{-1}. ICP: Pt:Au:P = 1.0:6.00:6.89. FABMS: obsvd *m/z* 3540.3 {calcd 3540.4 for $[(PPh_3)Pt(AuPPh_3)_6(HgI) = M]^+$}, 3408.8 {calcd 3408.6 for $[(PPh_3)Pt(AuPPh_3)_5(HgI)_2]^+$} (see discussion for explanation), 3213.0 {calcd 3212.9 for $[M - (HgI)]^+$}, 3077.3 {calcd 3077.5 for $[M - (PPh_3Hg)]^+$}, 3012.6 {calcd 3012.6 for $[M + (NO_3) - (HgIPPh_3)]^+$}, 2950.6 {calcd 2950.6 for $[M - (HgIPPh_3)]^+$}.

$[(PPh_3)Pt(AuPPh_3)_6(HgCo(CO)_4)](NO_3)$ (3(NO_3)). A Schlenk flask was charged with 52 mg (0.015 mmol) of 1(NO_3) and 4.0 mg (0.021 mmol) of $NaCo(CO)_4$ at −50 °C (dry ice/isopropyl alcohol bath) and cold, freshly distilled THF (10 mL) added. The reaction mixture was allowed to warm to room temperature with rapid stirring over the course of 1 h at which point the cloudy orange suspension was filtered through diatomaceous earth and the filtrate evaporated to dryness under reduced pressure. An orange-red precipitate formed after dissolution of the residue in 1 mL of acetone. The red solid was collected and washed with 3 × 1 mL of Et_2O before drying *in vacuo*. Yield: 23 mg (45%). The red solid is soluble in halogenated solvents, CH_3CN, CH_3OH, and acetone and insoluble in saturated hydrocarbons and diethyl ether. IR: ν(CO) 2039 cm^{-1} (sharp), 1952 cm^{-1} (br), 1884 cm^{-1} (br), $\nu(NO_3)$ 1340 cm^{-1} (br). ^{31}P NMR: δ 48.4 (doublet with ^{195}Pt and ^{199}Hg satellites, $^3J_{P-P}$ = 35.5 Hz, $^2J_{^{195}Pt-P}$ = 480 Hz, $^3J_{^{199}Hg-P}$ = approx. 480 Hz, int = 6), δ 65.4 (septet with ^{195}Pt satellites $^3J_{P-P}$ = 35.5 Hz, $J_{^{195}Pt-P}$ = 2580 Hz, $^2J_{^{199}Hg-P}$ unobserved, int = 1). FABMS: obsvd *m/z* 3584.5 calcd for $[(PPh_3)Pt(AuPPh_3)_6(HgCo(CO)_4) = M]^+$ unobserved, 3496.4 {calcd 3496.8 for $[(PPh_3)Pt(AuPPh_3)_5(HgCo(CO)_4)_2]^+$} (see discussion for explanation), 3212.6 {calcd 3212.9 for $[M - (HgCo(CO)_4)]^+$}, 3063.3 {calcd 3063.1 for $[Pt(AuPPh_3)_5Hg_2Co(CO)_4]^+$}, 3012.2 {calcd 3012.6 for $[M + (NO_3) - (HgCo(CO)_4PPh_3)]^+$}, 2950.3 {calcd 2950.6 for $[M - (HgCo(CO)_4PPh_3)]^+$}, 2753.0 {calcd 2753.6 for $[M - (AuPPh_3HgCo(CO)_4)]^+$}, 2687.9 {calcd 2687.9 for $[M - (HgCo(CO)_4(PPh_3)_2)]^+$}.

$[(PPh_3)Pt(AuPPh_3)_5(HgCo(CO)_4)_2](NO_3)$ (4(NO_3)). A Schlenk flask was charged with 0.190 g (0.057 mmol) of $[(PPh_3)Pt(AuPPh_3)_5(HgNO_3)_2](NO_3)$ and 0.0276 g (0.142 mmol) of $NaCo(CO)_4$, and cooled to −60 °C (dry ice/acetone bath). Freshly distilled THF (15 mL) was then added with stirring. The reaction mixture darkened from orange to a light cherry-red within several min and was warmed to 0 °C. After a total reaction time of 1.5 h, the slightly cloudy, cherry-red solution was evaporated to dryness under reduced pressure. The red residue was dissolved in CH_2Cl_2 (10 mL) and filtered through diatomaceous earth. The clear cherry red filtrate was reduced in volume to approximately 3 mL and an excess (20 mL) of Et_2O added with stirring. The resulting orange-red precipitate was collected on a fritted glass filter, washed with 3 × 5 mL portions of Et_2O, and dried *in vacuo*. Yield 0.1600 g (79%). The orange-red powder is soluble in halogenated solvents, CH_3CN, CH_3OH, and acetone and insoluble in saturated hydrocarbons and diethyl ether. ^{31}P NMR: (CD_2Cl_2, 20 °C) δ 56.3 (sextet with ^{195}Pt satellites, $^3J_{P-P}$ = 36.6 Hz, $J_{^{195}Pt-P}$ = 2644 Hz, $^2J_{^{199}Hg-P}$ unobserved, int = 1), δ 48.4 (doublet with ^{195}Pt and ^{199}Hg satellites, $^3J_{P-P}$ = 36.6 Hz, $^2J_{^{195}Pt-P}$ = 435 Hz, $^3J_{^{199}Hg-P}$ = 435 Hz, int = 5). IR: ν(CO) 2045 (sharp), 1949 (br), 1884 cm^{-1} (br), $\nu(NO_3)$ 1340 cm^{-1} (br) (unbound). FABMS: obsvd *m/z* 3496.9 {calcd 3496.8 for $[(PPh_3)Pt(AuPPh_3)_5(HgCo(CO)_4)_2] = M]^+$}, 2753.8 {calcd 2753.7 for $[M - 2(HgCo(CO)_4)]^+$}, 2665.9 {calcd 2665.9 for $[M - (HgCo(CO)_4AuPPh_3)]^+$}, 2491.5 {calcd 2491.4 for $[M - ((HgCo(CO)_4)_2PPh_3)]^+$}, 2295.3 {calcd 2294.4 for $[M - ((HgCo(CO)_4)_2\text{-}AuPPh_3)]^+$}.

Reaction of CO with 1(NO_3). CO was bubbled through a solution of 1(NO_3) (15 mg in 0.7 mL of CD_3OD) and the color immediately changed from clear red to orange with the precipitation of metallic Hg. After 5 min of reaction, ^{31}P NMR showed the presence of only $[(PPh_3)(CO)Pt(AuPPh_3)_6]^{2+}$,[25] indicating a clean displacement of Hg by CO. IR analysis of the solution confirmed this assignment (ν(CO) = 1967 cm^{-1}).[5] The reaction of $[(PPh_3)(CO)Pt(AuPPh_3)_6]^{2+}$ (67 mg in 12 mL acetone) with metallic Hg (80 mg) for 3 h yielded, by ^{31}P NMR, a mixture of 40% $[(PPh_3)(CO)Pt(AuPPh_3)_6]^{2+}$ and 60% 1, indicating that the bound CO ligand can also be displaced by Hg^0, although not completely within several hours.

X-ray Structure Determination for $[(PPh_3)Pt(AuPPh_3)_6(HgNO_3)](NO_3)$ (1(NO_3)). Collection and Reduction of X-ray Data. A summary of crystal data for 1 is presented in Table 1. The crystals rapidly lost solvent at room temperature, which rendered them unsuitable for X-ray diffraction. The crystal selected for data collection was therefore coated with a high molecular weight hydrocarbon, attached to the end of a glass fiber, and rapidly cooled to −100 °C in the cold nitrogen stream of the diffractometer. Data were collected at this temperature. The crystal class and space group were unambiguously determined by the Enraf-Nonius CAD4 peak search, centering, and indexing programs[26] and by successful solution and refinement of the structure (vide infra). Intensity data were collected by using monochromatized Mo Kα radiation (λ = 0.710 69 Å). A total of 15 354 reflections were collected of which 7722 were considered as observed with $I > 2.0\sigma(I)$. The intensities of three standard reflections were measured every 1.5 h of X-ray exposure time during data collection and no decay was noted. The data were corrected for Lorentz, polarization, and background effects. An empirical absorption correction was applied by use of the program DIFABS.[27] All data were collected using an Enraf-Nonius CAD-4 diffractometer with controlling hardware and software,[26] and all calculations were performed using the Molecular Structure Corporation TEXSAN crystallographic software package,[28] run on a Microvax 3 computer.

Solution and Refinement of the Structure. The structure was solved by direct methods.[29,30] Full-matrix least-squares refinement and difference Fourier calculations were used to locate the remaining non-hydrogen atoms. The atomic scattering factors were taken from the usual tabulation[31] and the effects of anomalous dispersion were included in F_c

Table 1. Crystallographic Data for $[(PPh_3)Pt(AuPPh_3)_6(HgNO_3)](NO_3)\cdot(C_2H_5)_2O\cdot(CH_3)_2CO$

Crystal Parameters and Measurement of Intensity Data	
space group	$P2_1/c$ (No. 14)
cell params at *T*, °C	−100
a, Å	24.968(7)
b, Å	15.848(9)
c, Å	30.60(1)
β, deg	92.69(3)
V, Å^3	12,093
Z	4
calcd density, g cm^{-3}	2.015
abs coeff, cm^{-1}	98.1
max, min transm factors	1.69, 0.78
formula	$C_{133}H_{121}N_2O_8P_7Au_6PtHg$
fw, amu	3669.72
Refinement by Full-Matrix Least Squares	
R^a	0.077
$R_w{}^a$	0.071

^{a} The function minimized was $\sum w(|F_o| - |F_c|)^2$, where $w = 4F_o^2/s^2(F_o)^2$. The unweighted and weighted residuals are defined as $R = \sum(||F_o| - |F_c||)/\sum|F_o|$ and $R_w = [(\sum w(|F_o| - |F_c|)^2)/(\sum w|F_o|^2)]^{1/2}$.

(26) Schagen, J. D.; Straver, L.; van Meurs, F.; Williams, G. Enraf-Nonius Delft, Scientific Instruments Division, Delft, The Netherlands, 1988.
(27) Walker, N.; Stuart, D. *Acta Crystallogr.* **1983**, *A39*, 158.
(28) All calculations were carried out with use of the Molecular Structure Corporation *TEXSAN-TEXRAY Structure Analysis Package*, version 2.1 **1985**.
(29) MITHRIL (an integrated direct methods computer program). University of Glascow, Scotland: Gilmore, C. J. *J. Appl. Crystallogr.* **1984**, *17*, 42.

Table 2. Positional Parameters and Their Esd's for the Core Atoms in $1(NO_3)$[a]

atom	x	y	z	B, Å²
Pt	0.69972(5)	0.00539(8)	0.18708(5)	0.87(6)
Au2	0.75006(5)	0.12106(9)	0.23566(5)	1.35(7)
Au3	0.67237(5)	0.00924(9)	0.27119(5)	1.30(7)
Au4	0.76047(5)	-0.08227(9)	0.24491(5)	1.30(7)
Au5	0.80198(5)	0.0311(1)	0.17255(5)	1.65(7)
Au6	0.72577(5)	0.0068(1)	0.10211(5)	1.39(7)
Au7	0.70093(6)	0.15504(9)	0.14779(6)	1.57(7)
Hg	0.61059(5)	0.0960(1)	0.19826(6)	1.86(8)
P	0.6527(3)	-0.1110(6)	0.1641(3)	1.5(5)
P2	0.7809(3)	0.2373(6)	0.2728(3)	1.3(5)
P3	0.6347(3)	0.0135(6)	0.3381(3)	1.5(5)
P4	0.8063(3)	-0.1799(6)	0.2870(4)	1.5(5)
P5	0.8922(3)	0.0292(6)	0.1689(3)	1.4(5)
P6	0.7412(4)	-0.0186(6)	0.0299(3)	1.7(5)
P7	0.6813(4)	0.2819(6)	0.1163(3)	1.4(5)
O1	0.516(1)	0.132(2)	0.202(1)	4.9(7)
O2	0.439(1)	0.084(2)	0.178(1)	5.8(8)
O3	0.507(1)	0.086(2)	0.135(1)	4.7(7)
N1	0.491(2)	0.100(3)	0.169(2)	6(1)

[a] Counterion, solvent molecule, and phenyl group positional parameters are provided in the supplementary material. Anisotropically refined atoms are given in the form of the isotropic equivalent thermal parameter defined as $(4/3)[a^2\beta(1,1) + b^2\beta(2,2) + c^2\beta(3,3) + ab(\cos\gamma)\beta(1,2) + ac(\cos\beta)\beta(1,3) + bc(\cos\alpha)\beta(2,3)]$.

by using Cromer and Ibers' values of $\Delta f'$ and $\Delta f''$.[32] The platinum, mercury, and phosphorus atoms were refined with anisotropic thermal parameters. The phenyl carbon atoms were refined as rigid groups with fixed geometry. The orientations and temperature factors of these groups were allowed to refine. Rigid group refinement of phenyl rings is often used with large clusters of this type as disorder in the ligands is common and has little effect on the geometry of the metal core. Phenyl hydrogen atoms were included in their idealized positions. The final positional and thermal parameters of the refined atoms within the coordination core are given in Table 2. An ORTEP drawing of the cluster core including the labeling scheme is shown in Figure 1. Table 3 gives selected distances and angles within the cluster core. A complete listing of crystallographic data, thermal and positional parameters, distances, and angles are included as supplementary material.[33]

Results

Synthesis and Characterization. The transformations observed in this study are summarized in the Scheme 1 and described in the Experimental Section. Characterization data for all new compounds are included in the Experimental Section and discussed in the next section when necessary. The reaction of the 16-electron compound $[(PPh_3)Pt(AuPPh_3)_6](NO_3)_2$ with 1 equiv of the Hg(I) compound $Hg_2(NO_3)_2(H_2O)_2$ has been previously reported and gives the 18-electron cluster $[(PPh_3)Pt(AuPPh_3)_5(HgNO_3)_2](NO_3)$.[5] The other product of this reaction is $(PPh_3)AuNO_3$. The reaction of an excess of metallic Hg with $[(PPh_3)Pt(AuPPh_3)_6](NO_3)_2$ in acetone solution gives the new cluster $[(PPh_3)Pt(AuPPh_3)_6(HgNO_3)](NO_3)$ ($\mathbf{1}(NO_3)$) in good yield. This 18-electron $PtAu_6Hg$ cluster has been characterized in the solid state by single-crystal X-ray diffraction (vide infra). Compound **1** reacts with the halide ions Cl^-, Br^-, and I^- in methanol solution to give the HgX analogues of **2** as shown in Scheme 1. These compounds are formed in good yield and were characterized by analytical and spectroscopic methods. Metallic Hg can be rapidly and cleanly displaced from **1** by reaction with CO (1 atm) in methanol solution to give the known compound $[(PPh_3)(CO)Pt(AuPPh_3)_6](NO_3)_2$.[25] The PtAuHg clusters **1** and $[(PPh_3)Pt(AuPPh_3)_5(HgNO_3)_2]^+$ react with $NaCo(CO)_4$ in THF solution to give the new tetrametallic compounds **3** and **4**, respectively. These PtAuHgCo clusters were characterized by analytical and spectroscopic methods.

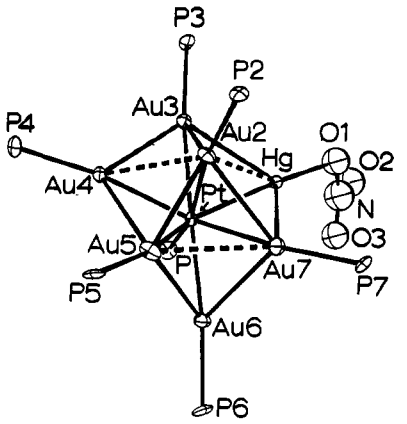

Figure 1. ORTEP drawing of the coordination core of $1(NO_3)$. Ellipsoids are drawn with 50% probability boundaries, and phenyl rings have been omitted for the sake of clarity.

Table 3. Selected Bond Lengths (Å) and Bond Angles (deg) with Esd's for the Cluster Core of $1(NO_3)$

Bond Lengths			
Pt–Au2	2.641(2)	Hg–Au2	3.636(3)
Pt–Au3	2.694(2)	Hg–Au3	2.988(2)
Pt–Au4	2.667(2)	Hg–Au7	2.945(3)
Pt–Au5	2.644(2)	Au2–Au3	2.878(2)
Pt–Au6	2.710(2)	Au2–Au4	3.244(2)
Pt–Au7	2.660(2)	Au2–Au5	2.770(2)
Pt–Hg	2.684(2)	Au2–Au7	2.952(3)
Pt–P	2.280(9)	Au3–Au4	2.785(2)
Au2–P2	2.279(9)	Au4–Au5	3.070(2)
Au3–P3	2.29(1)	Au5–Au6	2.834(2)
Au4–P4	2.28(1)	Au5–Au7	3.258(2)
Au5–P5	2.260(9)	Au6–Au7	2.818(2)
Au6–P6	2.30(1)	N–O1	1.26(6)
Au7–P7	2.27(1)	N–O2	1.36(5)
Hg–O1	2.45(1)	N–O3	1.17(6)
Hg–O3	3.16(1)		
Bond Angles			
Au2–Pt–P	163.7(3)	Pt–Au2–P2	169.2(2)
Au3–Pt–Au6	178.06(7)	Pt–Au3–P3	170.5(2)
Hg–Pt–Au2	86.13(6)	Pt–Au4–P4	168.8(3)
Hg–Pt–Au3	67.50(7)	Pt–Au5–P5	168.1(3)
Hg–Pt–Au4	130.05(6)	Pt–Au6–P6	168.7(3)
Hg–Pt–Au5	138.76(6)	Pt–Au7–P7	166.8(2)
Hg–Pt–Au6	110.84(7)	Pt–Hg–O1	160.5(5)
Hg–Pt–Au7	66.90(6)	Hg–O1–N1	108(1)
Hg–Pt–P	93.1(3)	O1–N1–O2	112(4)
Au4–Pt–Au2	75.36(7)	O1–N1–O3	128(4)
Au4–Pt–Au3	62.59(6)	O2–N1–O3	121(4)
Au4–Pt–Au5	70.62(6)	Au4–Pt–Au7	138.28(7)
Au4–Pt–Au6	119.10(7)		

Crystal Structure of $1(NO_3)\cdot(C_2H_5)_2O\cdot(CH_3)_2CO$. Selected positional parameters and interatomic distances and angles are given in Tables 2 and 3, respectively. The molecular structure of the coordination core together with the crystallographic numbering scheme is given in Figure 1. Additional data is provided as supplementary material.[33] The NMR data indicate that Pt is in the center of the $PtAu_6Hg$ skeleton, the metal atoms connected to PPh_3 ligands are Au, and the metal atom connected to the nitrate ligand is Hg. This is consistent with other Hg adducts of PtAu clusters.[5,14]

The cluster core of **1** has an unusual geometry that is best described as being between the limits of a Pt-centered, icosahedral fragment (as in $[(PPh_3)Pt(AuPPh_3)_5(HgNO_3)_2]^+$)[5] and a cube

(30) DIRDIF (direct methods for difference structures; an automatic procedure for phase extension and refinement of difference structure factors): Beurskens, P. T. *Technical Report 1984/1*; Crystallography Laboratory: Toernooiveld, 6525 ED Nijmegen, The Netherlands, 1984.
(31) Cromer, D. T.; Waber, J. T. In *International Tables for X-Ray Crystallography*; Kynoch: Birmingham, England, 1974; Vol. IV, Table 2.2 A.
(32) Cromer, D. T. In *International Tables for X-Ray Crystallography*; Kynoch: Birmingham, U. K., 1974; Vol. IV, Table 2.3.1. Ibers, J. A.; Hamilton, W. C. *Acta Crystallogr.* **1964**, *17*, 781.
(33) See paragraph at the end of the paper regarding supplementary material.

Scheme 1

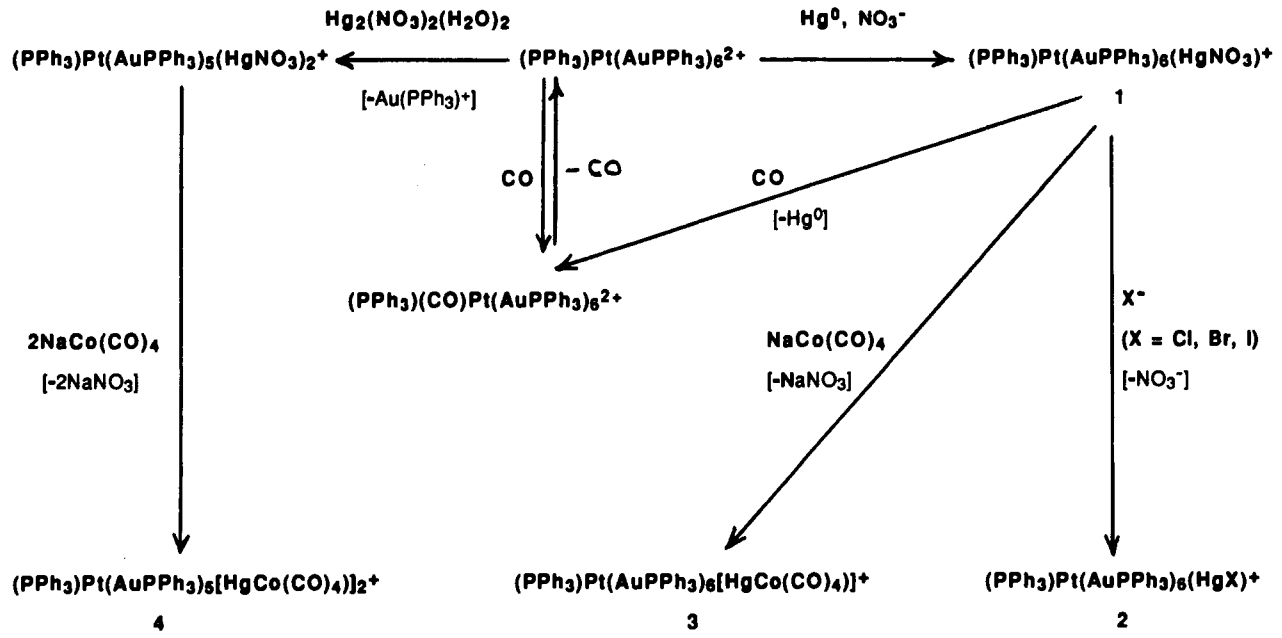

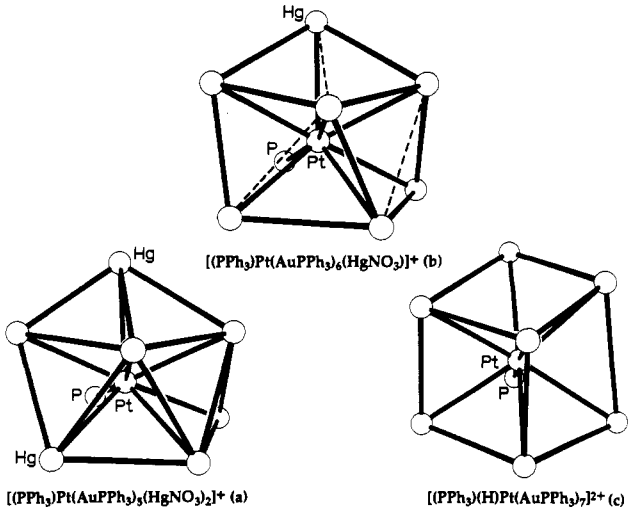

Figure 2. PLUTO drawings of the cluster $PPtM_7$ cores of $[(PPh_3)Pt(AuPPh_3)_5(HgNO_3)_2]^+$ (a), $[(PPh_3)Pt(AuPPh_3)_6(HgNO_3)]^+$ (b), and $[(PPh_3)(H)Pt(AuPPh_3)_7]^{2+}$ (c) showing the geometry change from an icosahedral fragment to a distorted cube. The gold atoms are shown without labels.

(as in $[(PPh_3)(H)Pt(AuPPh_3)_7]^{2+}$).[13] Figure 2 shows PLUTO drawings of the metal frames of these three clusters. In $[(PPh_3)Pt(AuPPh_3)_5(HgNO_3)_2]^+$ (Figure 2a) the geometry is best represented as that of an icosahedral fragment.[5] All peripheral M_3 units in this cluster form approximate equalateral triangles and the peripheral metal atoms are close to the vertex positions of a centered icosahedron. In $[(PPh_3)(H)Pt(AuPPh_3)_7]^{2+}$ (Figure 2c) the peripheral gold atoms form approximately square, planar faces and the structure is close to a cube if the phosphorus atom of the Pt bound PPh_3 ligand is included. The only other PtAu cluster with this cubic geometry is $[(PPh_3)(C{\equiv}C\text{-}t\text{-}Bu)Pt(AuPPh_3)_6]^+$.[34] The structure of **1** is between these limits. The peripheral M-M distances shown in Figures 1 and 2b with dashed lines (Hg–Au2, 3.636 Å; Au2–Au4, 3.244 Å; Au5–Au7, 3.258 Å) are significantly elongated compared with the ones with solid lines (average 2.893 Å, range 2.770–3.070 Å) giving distorted, nonplanar square faces. The average nearest peripheral M–M distance in the icosahedral fragment cluster $[(PPh_3)Pt(AuPPh_3)_5(HgNO_3)_2]^+$ is 2.931 Å (range 2.775–3.072 Å) which is close to the distances with solid lines in **1**. In $[(PPh_3)(H)Pt(AuPPh_3)_7]^{2+}$, the average Au–Au distance defining the nearly planar, square faces is 2.889 Å (range 2.820–3.074 Å) while the diagonals of the square faces are much longer (average 4.27 Å).[13] Although the distorted geometry of **1** is different from that observed in other 18-electron PtAu clusters, it is spheroidal in agreement with its 18-electron count.

The only other PtAuHg clusters which have been characterized by X-ray diffraction are $[(PPh_3)Pt(AuPPh_3)_5(HgNO_3)_2](NO_3)$[5] and $[Pt(AuPPh_3)_8Hg_2](NO_3)_4$.[14] A comparison of the distances within the metal cores of these clusters is presented in Table 4. The Pt–Hg distance in **1** is similar to the distances in $[(PPh_3)Pt(AuPPh_3)_5(HgNO_3)_2](NO_3)$ and within the wide range of values found in dinuclear PtHg compounds (2.51–2.83Å),[36] but significantly shorter than in $[Pt(AuPPh_3)_8Hg_2](NO_3)_4$ and the Pt_3Hg clusters (average 2.99 Å),[17,35] The Pt-Hg distances in all of the clusters, however, are longer than the sum of the covalent radii of Pt and Hg (2.532 Å).[37] The nearest neighbor Hg–Au distances in **1** are similar to values found in the other PtAuHg clusters and are similar to the nearest neighbor Au–Au distances indicating that the Hg and Au atoms have similar bonding properties in these compounds. The Pt–Au distances in **1** are similar to values in the other PtAuHg clusters (Table 4) and are within the range of values observed in PtAu clusters containing primarily phosphine ligands.[1-5] The Au–P and Pt–P bond lengths are also in the range normally found in gold and mixed-metal–gold clusters.[1-5] The nitrate is bound to the Hg atom in an unsymmetrical fashion with Hg–O distances of 2.45 and 3.16 Å. The shorter Hg–O vector is approximately trans to the Hg–Pt vector (Pt–Hg–O angle 160.5°). The Au–P vectors are also approximately trans to the Au–Pt vectors (average Pt–Au–P angle 168.7°) as generally found in gold phosphine clusters.[1-5]

Discussion

The reaction of $Hg_2(H_2O)_2(NO_3)_2$ with $[(PPh_3)Pt(AuPPh_3)_6]^{2+}$ gives the dimercury cluster compound $[(PPh_3)Pt(AuPPh_3)_5(HgNO_3)_2]^+$.[5] This reaction increases the coordination number

(34) Smith, E. W.; Welch, A. J.; Treurnicht, I.; Puddephatt, R. J. *Inorg. Chem.* **1986**, *25*, 4616.

(35) Yamamoto, Y.; Yamazaki, H.; Sakurai, T. *J. Am. Chem. Soc.* **1982**, *104*, 2329.

(36) Krumm, M.; Zangrando, E.; Randaccio, L.; Menzer, S.; Danzmann, A.; Holthenrich, D.; Lippert, B. *Inorg. Chem.* **1993**, *32*, 2183 and references cited therein.

(37) Ghilardi, C. A.; Midollini, S.; Moneti, S.; Orlandini, A.; Scapacci, G.; Dakternieks, D. *J. Chem. Soc., Chem. Commun.* **1989**, 1686.

Table 4. Comparison of Bond Distances (Å)[a] in Pt–Au–Hg Cluster Compounds

	$[Pt(AuPPh_3)_8(Hg)_2]^{4+}$ [b]	$[(PPh_3)Pt(AuPPh_3)_5(HgNO_3)_2]^+$ [c]	$[(PPh_3)Pt(AuPPh_3)_6(HgNO_3)]^+$
Hg–Pt	2.928, 3.045	2.651, 2.667	2.684
Hg–Au	av 3.004 (3.007–3.001)	av 2.951 (2.775–3.072)	av 3.190 (2.945–3.636)
Pt–Au	av 2.632 (2.631–2.632)	av 2.680 (2.647–2.705)	av 2.669 (2.641–2.710)
Au–Au	av 3.135 (2.904–3.380)	av 2.906 (2.811–3.056)	av 2.956 (2.770–3.258)
Au–P	av 2.292 (2.289–2.295)	av 2.280 (2.27–2.299)	av 2.280 (2.260–2.30)
Pt–P		2.284	2.280
Hg–O		2.28, 2.66; 2.32, 2.62	2.45, 3.16

[a] Values in parentheses show the range of observed bond lengths. [b] Reference 14. [c] Reference 5.

of the central Pt atom by one ($AuPPh_3^+$ is lost during this reaction) and the number of valence electrons of the metal frame by two. It is similar to the addition of $Hg_2(H_2O)_2(NO_3)_2$ to $[Pt(AuPPh_3)_8]^{2+}$ which gives the dimercury cluster $[Pt(AuPPh_3)_8(Hg)_2(NO_3)_2]^{2+}$.[14] Both reactions involve the addition of a $Hg_2(NO_3)_2$ moiety to a 16-electron cluster to give a dimercury 18-electron cluster, with the expected change from toroidal to spheroidal symmetry of the metal frame. The reaction of metallic Hg with $[(PPh_3)Pt(AuPPh_3)_6]^{2+}$ yields the new monomercury adduct **1**. This reaction involves the simple addition of one Hg atom with its two valence electrons to give $[(PPh_3)Pt(AuPPh_3)_6(Hg)]^{2+}$, thus increasing the coordination number by one and the electron count to 18. In the solid state one of the nitrate counter ions is bound to the Hg atom, while in solution this anion is dissociated as determined by its conductivity (see Experimental Section). In agreement with this electron count, the metal frame symmetry of **1** is spheroidal as determined by X-ray diffraction (Figure 1). ^{31}P NMR, FABMS, and elemental analysis data are consistent with the formulation of **1**.

We have been unable to prepare this monomercury cluster compound from $[(PPh_3)Pt(AuPPh_3)_6]^{2+}$ by reaction with Hg(I) or Hg(II) compounds. Since the reaction of Hg(0) leads to different PtAuHg clusters, it opens up new synthetic possibilities in PtAu cluster chemistry. We are currently exploring this reaction with other PtAu and PdAu cluster compounds with good success.[38] Compound **1** reacts with CO to give the known carbonyl adduct $[(PPh_3)(CO)Pt(AuPPh_3)_6]^{2+}$ and metallic Hg. This reaction is reversible in that the readdition of Hg to $[(PPh_3)(CO)Pt(AuPPh_3)_6]^{2+}$ leads to formation of **1**, probably through $[(PPh_3)Pt(AuPPh_3)_6]^{2+}$ as an intermediate. This reversible addition of Hg(0) is similar to reactions observed by Puddephatt[15] for $[Pt_3(\mu_3\text{-}CO)(\mu\text{-}dppm)_3]^{2+}$ and by McPartlin[16] for $[Os_{18}Hg_2C_2(CO)_{42}]^{2-}$, although the latter example involves the photochemical loss of Hg.

The nitrate group bound to the Hg in **1** can be replaced by X^- (X = Cl, Br, I) in solution and isolated as the halide derivatives **2**, X. These derivatives have been characterized in solution by ^{31}P NMR (see supplementary material),[33] ICP, conductivity, IR, and FABMS analysis (see Experimental Section). These data are completely consistent with their formulation. All of the clusters are fluxional and show only one Au–*P* chemical shift. This is typical of phosphine stabilized PtAu and Au cluster compounds.[1-5]

The NMR coupling constants in this series of compounds show an interesting trend. The values of the P–Pt coupling constants ($^2J_{^{195}Pt-P}$, $J_{^{195}Pt-P}$) for the compounds $[(PPh_3)Pt(AuPPh_3)_6]^{2+}$, $[(PPh_3)(CO)Pt(AuPPh_3)_6]^{2+}$, **1**, **2**, X = Cl, **2**, X = Br, and **2**, X = I are as follows: 413, 3766; 385, 2469; 462, 3670; 468, 2813; 470, 2830; and 471, 2813, respectively. The CO adduct of $[(PPh_3)Pt(AuPPh_3)_6]^{2+}$ has significantly lowered Pt–P and Pt–Au–P coupling constants, indicating a weakening of the Pt–P and Pt–Au–P bonding relative to $[(PPh_3)Pt(AuPPh_3)_6]^{2+}$. The Hg adduct, **1**, has a significantly increased *Pt*–Au–*P* coupling constant relative to $[(PPh_3)Pt(AuPPh_3)_6]^{2+}$, indicating a strengthening of the Pt–Au–P bonding, even though the coordination number of the Pt is increased by one just as in the CO adduct. The effect of Hg on the Pt–Au bonding is therefore very different from that of CO. Although the *Pt*–Au–*P* ^2J values in the halide derivatives **2**, X, are similar to that in **1**, the Pt–P ^1J values decrease significantly by about 850 Hz. It is unclear why this occurs. An even greater lowering of J_{Pt-P} was observed in the carbonyl adduct $[(PPh_3)(CO)Pt(AuPPh_3)_6]^{2+}$. The *Hg*–Pt–Au–*P* coupling constants ($^3J_{^{199}Hg-P}$) for the series **1**, **2**, X = Cl, **2**, X = Br, and **2**, X = I are 655, 566, 564, and 544 Hz, respectively. A similar trend has been observed in the series $[(PPh_3)Pt(AuPPh_3)_5(HgX)_2]^+$ where X = NO_3, Cl, Br, and I.[5] This trend is indicative of a strengthening of the Hg–X bonding in the order I > Br > Cl which decreases the overall Hg–Pt–Au–P bonding. This is reasonable because the soft I ligand is expected to bond better to a soft Hg atom than Br or Cl. The effect on cluster bonding of such electronic changes is complicated and not understood, but the trends observed above should help in future spectroscopic and theoretical studies on the electronic structure of these clusters.

Table 5. Comparison of Carbonyl Stretching Frequencies for $Co(CO)_4$ Adducts of Au and Au–Hg Compounds

compound	ν(CO) stretches,[a] cm^{-1}	ref
$[(PPh_3)Pt(AuPPh_3)_6(HgCo(CO)_4)](NO_3)$	2039, 1952, 1884	this work
$[(PPh_3)Pt(AuPPh_3)_5(HgCo(CO)_4)_2](NO_3)$	2045, 1949, 1884	this work
$[(AuPPh_3)_4(AuCo(CO)_4)_2]$	2010, 1940, 1885	*c*
$[(PPh_3)Au(Co(CO)_4)]$	2045, 1975, 1945	*c*
$[(PPh_3)Au(Co(CO)_4)]$	2054, 1988, 1957[b]	*d*

[a] CsI pellets. [b] CS_2 solution. [c] Reference 40. [d] Reference 41.

The FABMS data of the clusters **1** and **2** are consistent with their formulations, however, for compounds **2**, X = Br and I, we have observed peaks assigned to the ions $[(PPh_3)Pt(AuPPh_3)_5(HgX)_2]^+$ (see Experimental Section). Although we have frequently observed ions due to the addition of fragments of the *m*-nitrobenzyl alcohol matrix,[39] this is the first time we have observed ions due to the addition of an extra metal. We are confident that these compounds do not contain two mercury atoms as such derivatives are known and have different NMR spectra, which would be easy to detect.[5] The same phenomenon occurs with $[(PPh_3)Pt(AuPPh_3)_6(HgCo(CO)_4)]^+$ (**3**), where a peak assigned to $[(PPh_3)Pt(AuPPh_3)_5(HgCo(CO)_4)_2]^+$ is present. A possible explanation is that HgX dissociates in the heated matrix due to Xe atom bombardment and adds to another cluster, giving species with two Hg atoms. It is important to be aware that such reformulation of a compound can occur in the FABMS matrix, although such peaks are generally smaller than those due to more normal fragmentation.

The reactions of **1** and $[(PPh_3)Pt(AuPPh_3)_5(HgNO_3)_2]^+$ with $NaCo(CO)_4$ in THF solution give the new tetrametallic clusters $[(PPh_3)Pt(AuPPh_3)_6(HgCo(CO)_4)]^+$ (**3**), and $[(PPh_3)Pt(AuPPh_3)_5(HgCo(CO)_4)_2]^+$ (**4**), respectively. These compounds have been characterized by ^{31}P NMR, IR, and FABMS analysis. The ^{31}P NMR data for **3** are similar to those of compounds **1** and **2**,

(38) Gould, R. A. T.; Craighead, K. L.; Wiley, J.; Pignolet, L. H. To be submitted for publication in *Inorg. Chem.*

(39) Boyle, P. D.; Johnson, B. J.; Alexander, B. D.; Casalnuovo, J. A.; Gannon, P. R.; Johnson, S. M.; Larka, E. A.; Mueting, A. M.; Pignolet, L. H. *Inorg. Chem.* **1987**, *26*, 1346.

however, the trend in the Pt–P and *Hg*–Pt–Au–*P* coupling constants (**1** > **2** > **3**) indicates that the $Co(CO)_4$ group causes an increased weakening in the Pt–Au bonding (see discussion above) compared with the halide derivatives. This same trend is observed with **4** compared with its halide and nitrate derivatives.[5] The carbonyl stretching frequencies for **3** and **4** are tabulated in Table 5 along with values for some other well-characterized $Co(CO)_4$ adducts of Au compounds.[40,41] It is clear from the similarity of this data that compounds **3** and **4** contain $Co(CO)_4$ groups. In addition, there are several known examples of $Co(CO)_4$ bound to Hg and Pt in the heterometallic compounds $RuCo_3(CO)_{12}[\mu_3\text{-}HgCo(CO)_4]$[42] and $[(CO)_4CoHgPt(C_6Cl_5)(PPh_3)_2]$.[43] These compounds were prepared in a manner similar to that for **3** and **4** with use of $[Co(CO)_4]^-$ as a reagent. Compounds **3** and **4** are the first tetrametallic PtAu clusters and could prove useful in the preparation of larger polymetallic cluster compounds.

Acknowledgment. This work was supported by the National Science Foundation (Grants CHE-9222411 and 9121708) and by the University of Minnesota. We also acknowledge Jan Lane and Wayde V. Konze for help in the preparation of starting compounds, Prof. John E. Ellis for a gift of some $NaCo(CO)_4$, and Mrs. A. Roelofsen for performing ICP analyses.

Supplementary Material Available: Tables SI–SV, listing complete crystal data and data collection parameters, general temperature factor expressions, final positional and thermal parameters for all atoms, and distances and angles, and Figure S1, showing ^{31}P NMR spectra for compounds **1** and **2** (23 pages). Ordering information is given on any current masthead page.

(40) van der Velden, J. W. A.; Bour, J. J.; Bosman, Noordik, J. H. *Inorg. Chem.* **1983**, *22*, 1913.
(41) Coffey, C. E.; Lewis, J.; Nyholm, R. S. *J. Chem. Soc. A* **1971**, 1685.
(42) Braunstein, P.; Rose, J.; Tiripicchio, A.; Tiripicchio-Camellini, M. *J. Chem. Soc., Chem. Commun.* **1984**, 391.
(43) Calvet, J.; Rossell, O.; Seco, M.; Braunstein, P. *J. Chem. Soc., Dalton Trans.* **1987**, 119.